

THE SN Ia RATE AT $z=0.47$ FROM THE SNLS



J. D. Neill, D. Balam, C. Pritchett, M. Graham, E. Hsiao (University of Victoria), M. Sullivan, A. Howell,
K. Perrett, A. Conley, R. G. Carlberg (University of Toronto), P. Astier, J. Guy, R. Pain, N. Regnault, R. Tillet, S. Baumont (LPNHE),
E. Auborg (APC), S. Basa (LAM, CNRS), J. Bronder, I. Hook (Oxford), S. Fabbro, A. Mourao (CENTRA)
D. Fouchez, P. Ripoche, C. Tao (CPPM), H. Lafoux, N. Palanque-Delabrouille, J. Rich, V. Lussat (DSM/DAPNIA), S. Perlmutter (LBNL)



Constraining SN Ia Physics

Population synthesis models for different SN Ia scenarios predict different SN Ia production timescales, τ , relative to the input star formation history (SFH). By comparing the global rate of occurrence of SNe Ia at different redshifts to measurements of the global cosmic SFH, we can constrain τ and, hence, the physical process that leads to the SN Ia.

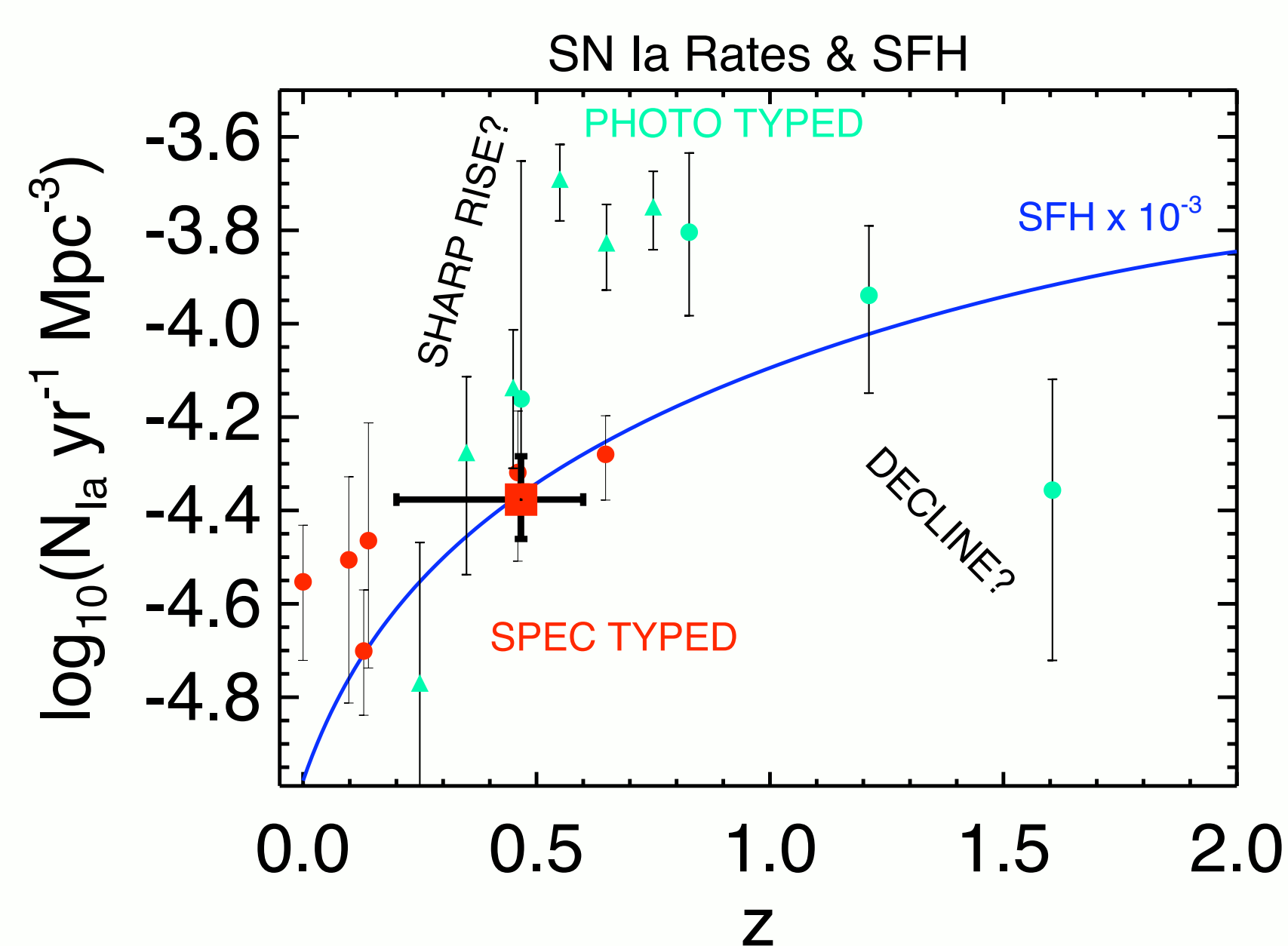


Figure 1: SN Ia rates from the literature compared with a recent SFH fit from Hopkins & Beacom (2006) scaled by a factor of 10^3 . The solid red points are from studies that used spectroscopic confirmation for their SN Ia sample (red references below). The turquoise symbols are from studies that used photometric typing (triangles, Barris & Tonry 2005) or a combination of low-resolution objective prism spectroscopy and photometric typing (circles, Dahlen et al. 2004). The red square is the SNLS value.

We immediately notice two significant features in the observed SN Ia rate evolution that have no analog in the SFH: the sharp rise near $z = 0.5$, and the decline beyond $z = 1.2$. Could these be due to systematics?

SNLS Efficiencies

The Supernova Legacy Survey (SNLS) is a well-characterized rolling search survey (see other posters in session 15) with excellent light curve coverage and spectroscopic followup making it ideal for determining SN Ia rates. We use the properties of the survey in the redshift range $0.2 < z < 0.6$ to define our object selection criteria. These criteria are applied to the full set of spectroscopically confirmed SNe Ia from the first two seasons of the SNLS to derive our observed sample of 58 objects. We then use the exact same criteria to calculate the survey efficiency using SNLS survey epochs in a Monte Carlo simulation that observes a realistic population of 10^6 simulated SNe Ia.

Table 1. % Efficiencies

Field	On-Field ^a		Yearly
	<i>i'</i> Detection ^b	Spec	
D1	95	61	30
D2	98	53	22
D3	97	63	31
D4	98	65	31

^aOn-Field is during the field's observing season

^bThe Canadian pipeline uses *i'* for detection

Spectroscopic Completeness

We are aided in our calculation of spectroscopic completeness by the rolling search method of our survey, which allows us to follow all variable objects in our fields and weed out objects with variation timescales inconsistent with SNe Ia (AGN, variable stars). We used complete light curves in all colors of all SN-type candidates to quantify the missed SNe Ia, *i.e.*, those that passed our selection criteria, but did not obtain spectroscopic followup.

Table 2. Spectroscopic Completeness

Field	SNe Ia			% Complete	
	Confirmed	Probable	Possible	Minimum	Most Likely
D1	16	1	4	76	94
D2	15	2	0	88	88
D3	16	4	2	73	80
D4	11	5	1	65	69
ALL	58	12	7	75	83

Results

We compare our efficiencies and the spectroscopic completeness with our sample to derive the SN Ia rate at the volume weighted average redshift of $z=0.47$. The table below shows the rate after each correction is made on the way to deriving the final volumetric SN Ia rate, which is an error weighted average over all four deep fields.

Table 3. Type Ia SN Volumetric Rate

r_{RAW} (yr^{-1})	r_{spec}^a (yr^{-1})	r_{1+z}^b (yr^{-1})	Ω degrees ²	V $\times 10^4$ Mpc ³	r_V ($\times 10^{-4} yr^{-1} Mpc^{-3}$)
24.1 ± 3.3	30.3 ± 4.0	44.4 ± 5.9	1.026	106.2	0.42 ± 0.06^c

^arate after correcting for spectroscopic incompleteness

^brate after correcting for time dilation

^cstatistical error only

Systematic Errors

The spectroscopic completeness calculation (above) and supplemental Monte Carlo experiments allow us to estimate the systematic uncertainties due to survey properties and errors in the SN Ia parameters that define the simulated population. Below is a table summarizing the most important sources of systematic error.

Table 4. Systematic Errors

Source	δr_V ($\times 10^{-4} yr^{-1} Mpc^{-3}$)
Spec. Completeness	+0.03 -0.08
Host Extinction	+0.10
Frame Limits	-0.03
Stretch	± 0.01
Total Systematic	+0.10 -0.09

References

- Barris, B. & Tonry, J. 2005 ApJ, in press, astro-ph/0509655
Blanc, G., et al. 2004, A&A, 423, 881
Cappellaro, E., Evans, R., & Turatto, M. 1999, A&A, 351, 459
Dahlen, T., et al. 2004, ApJ, 613, 189
Hardin, D., et al. 2000, A&A, 362, 419
Hopkins, A. M., & Beacom, J. F. 2006 in preparation
Madgwick, D. S., Hewett, P. C., Mortlock, D. J., & Wang, L. 2003, ApJ, 599, L33
Mannucci, F., et al. 2005, A&A, 433, 807
Pain, R., et al. 2002, ApJ, 577, 120
Riello, M., & Patat, F. 2005, MNRAS, 362, 671
Scannapieco, E. & Bildsten, L. 2005, ApJ, 629, L85
Tonry, J. L., et al. 2003, ApJ, 594, 1

Host Extinction

We used the recent dust models of Riello & Patat (2005) in supplemental Monte Carlo simulation runs to calculate the extent of our systematic error due to underestimating host extinction, our largest source of systematic error (see Table 4).

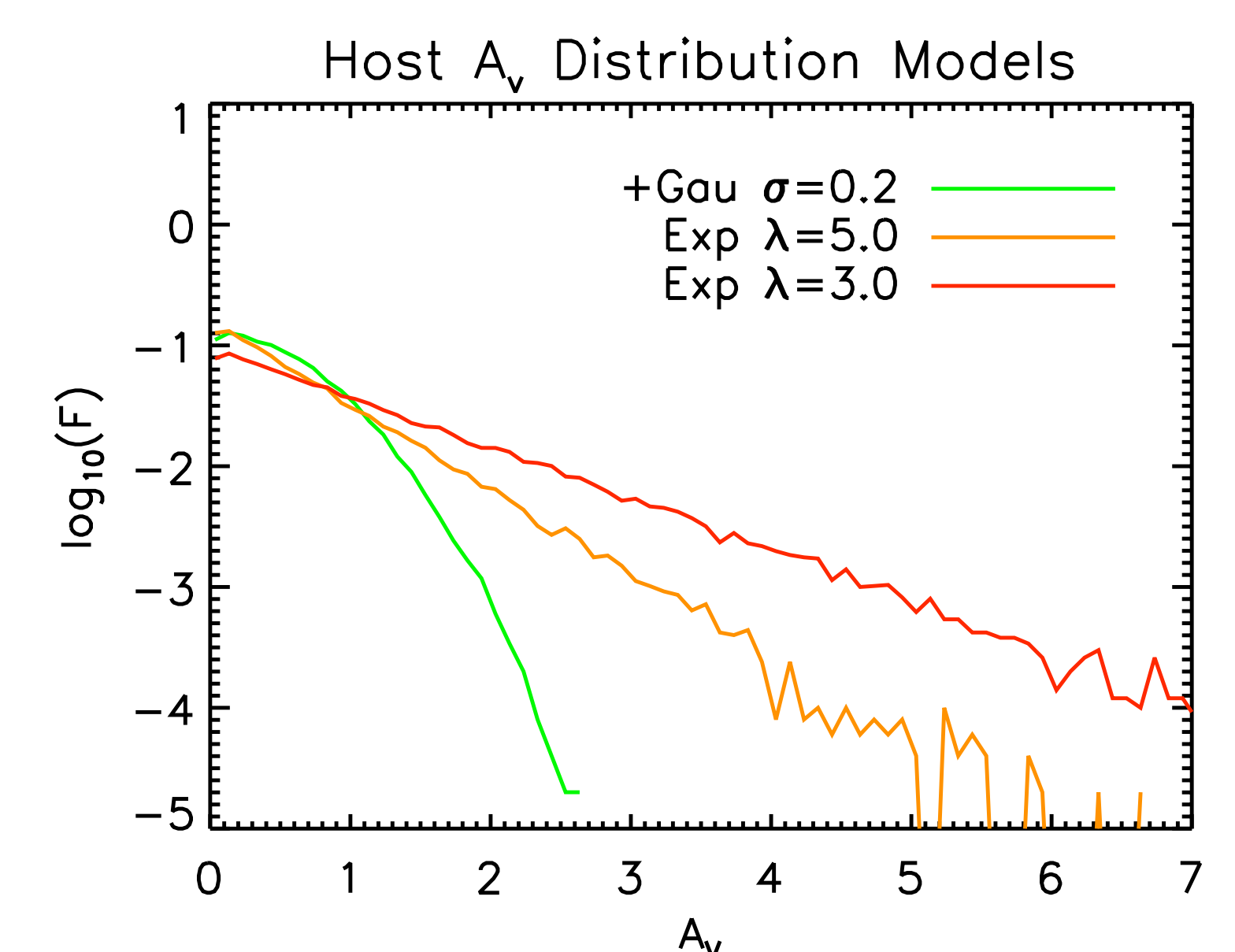


Figure 2: distributions of total V-band extinction for three models of SN Ia host extinction. Our canonical distribution is the green line. The orange and red lines are distributions with exponential tails reaching to much higher extinction.

Our canonical distribution is consistent with an intermediate host inclination model which is representative of hosts with random inclinations. The exponential distributions are consistent with extreme inclination models and bound the systematic error due to host extinction.

SFH Comparison

Using our rate and the spectroscopically confirmed rates from the literature combined with the SFH from Hopkins & Beacom (2006), we now constrain the two-component model of SN Ia production described in Scannapieco and Bildsten (2005, for details see poster 15.07). This model is composed of a component that tracks SFH (short τ) and a component that tracks integrated mass (long τ). It is motivated by the high SN Ia rate in star-forming galaxies and the non-zero rate in ellipticals (see, *e.g.*, Mannucci et al. 2005).

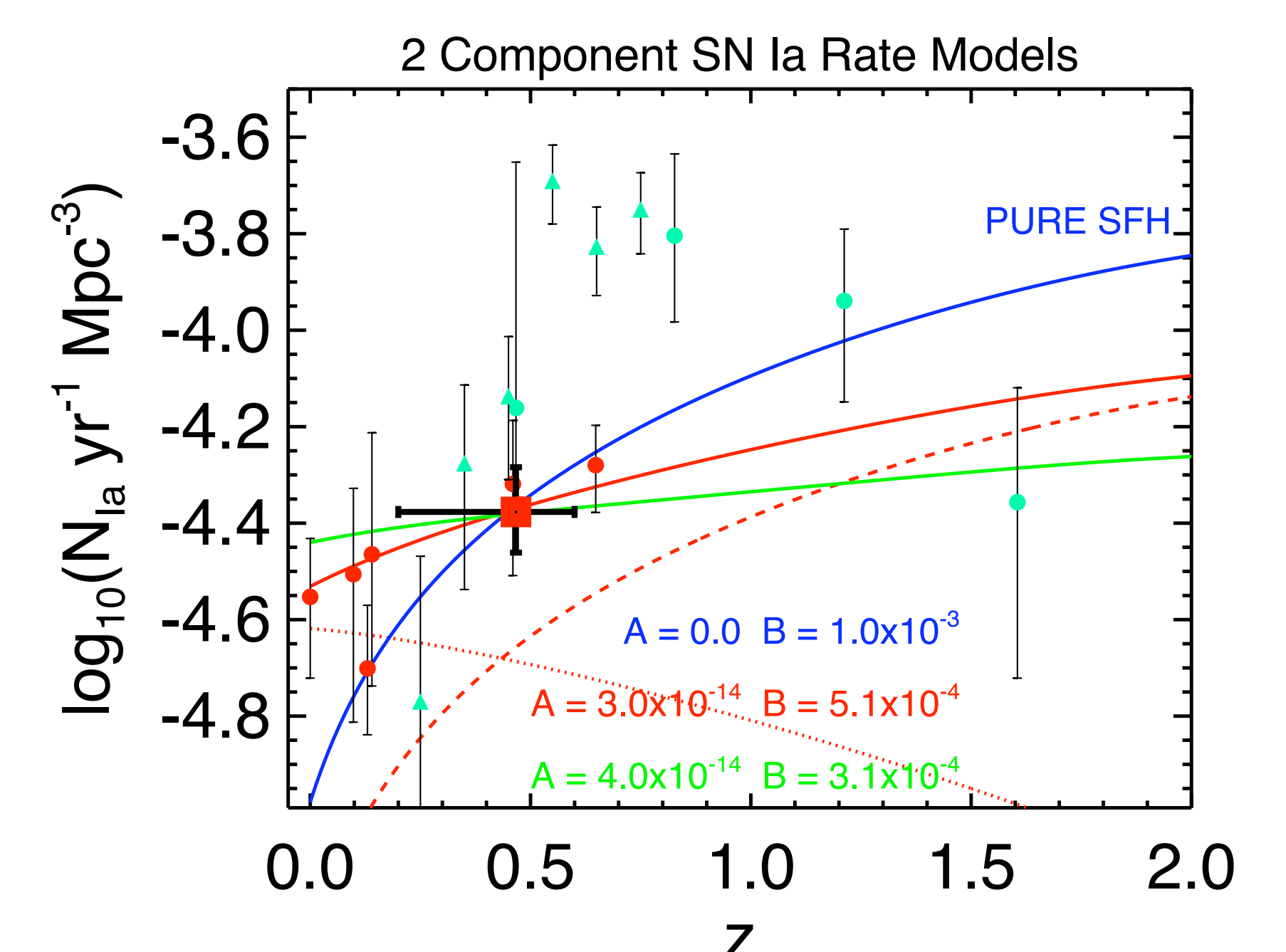


Figure 3: same as Figure 1, but with models of SN Ia production overplotted. The blue line is equivalent to a two-component model with an integrated mass component of zero. The red line is the two-component model that fits the volumetric rate evolution. Both components are shown for this model: the A component is the dotted red line and the B component is the dashed red line. The green line is the two-component model derived from fitting the SN Ia rate in individual galaxies as a function of mass and star formation rate (see poster 15.07).

Spectroscopically confirmed SN Ia rates show only modest evolution out to $z \sim 0.7$ and are consistent with the two-component model, which we constrain to have a SFH component (B) of less than 1 SN Ia per $\sim 10^3 M_{\odot}$ formed.